Wave propagation in a wavy fiber–epoxy composite material: Theory and experiment

Kwang Yul Kim, Wei Zou and Wolfgang Sachse

Wave propagation in a wavy fiber–epoxy composite material: Theory and experiment

Kwang Yul Kim,[a] Wei Zou, and Wolfgang Sachse

Department of Theoretical and Applied Mechanics, Thurston Hall, Cornell University, Ithaca, New York 14853-1503

In this paper analytic formulas are developed for the ray path and travel time of a ray propagating in a wavy fiber–epoxy composite material and calculate them for rays initiating at various points with wave normals of differing directions. The arrival times observed by using various combinations of pointlike sources and pointlike detectors are found in good agreement with those predicted by the theory of geometrical acoustics. © *1998 Acoustical Society of America.* [S0001-4966(98)04805-X]

PACS numbers: 43.20.Dk [ANN]

INTRODUCTION

Fiber-waviness is introduced in composite materials during manufacturing processes because of uneven curing and shrinkage of resin, and it has detrimental effects on mechanical properties, such as stiffness reduction and degradation of compressive strength.[1,2] Layer waviness also occurs in thick crossply or multidirectional laminates due to the lamination residual stresses built up during curing process. Therefore, it is important to detect and characterize fiber-waviness during and after fabrication of a fiber-reinforced composite, and nondestructive ultrasonic evaluation of the wavy composite remains a challenging problem.

There have been the investigations on the unidirectional wavy composite by means of ultrasonic waves. Wooh and Daniel[3] used a ray tracing method in an attempt to understand the waveforms detected by the piezoelectric transducers of finite size attached on one side of the flat surfaces. The waveforms were launched by the piezoelectric transducers of finite size on the same or opposite side of the flat surfaces. Using the finite difference method, McIntyre *et al.*[4] theoretically investigated the harmonic wave propagation with wave normal directed in the mean fiber-direction, and found the variation of amplitude in tune with the energy conservation principle implied by the transport equation.

In this paper we apply the results of geometrical acoustics to investigate ray paths and travel times along the various ray paths of ultrasonic waves propagating in a wavy graphite fiber–epoxy composite. Even though experimental verification of the theoretical ray paths is difficult to achieve because of the opaque composite specimen, it will be demonstrated that the observed travel times of the quasilongitudinal (QL) and shear horizontally (SH) polarized pure transverse (PT) modes propagating along the different ray paths are found in good agreement with those predicted by the theory of geometrical acoustics.

I. THEORY

A schematic diagram of a wavy composite specimen is drawn in Fig. 1, where the reinforcing fibers are running in a wavy pattern in the xy plane with their mean direction pointing along the x axis. We specify the waviness of the fiber-reinforced epoxy composite by the following sine wave function

$$y_f = A_f \sin(2\pi x/L_f), \qquad (1)$$

where y_f is the fiber height in the y direction, A_f is the amplitude of fiber-waviness, and L_f is the periodical length of waviness. A local fiber-direction is specified by the angle β_f the x axis makes with the fiber. Here, $\tan\beta_f$ is given by

$$\tan\beta_f = \frac{dy_f}{dx} = \frac{2\pi A_f}{L_f}\cos\frac{2\pi x}{L_f}. \qquad (2)$$

The imbedded wavy fibers notwithstanding, the fabricated wavy composite specimens are observed to have the uniform density ρ throughout the specimens, and we assume that the density of the wavy composite is constant. The wavy composite is also uniform along the z axis normal to the xy plane on which the waviness of the fibers is confined. The composite is also uniform along the y direction. As a result, both anisotropy and heterogeneity of the wavy composite is a function of one variable x only. Therefore, the wave normals, which are initially directed in the xy plane, are confined on the xy plane and refraction of the wave normals is governed by Snell's law during the propagation of rays in the xy plane. A composite material which has the fibers running straight in the x direction ideally has transversely isotropic symmetry about the x axis. However, because of a less-than-ideal fabrication procedure, it is better characterized as possessing weak orthorhombic symmetry with proximity to transverse isotropy. Let the x, y, and z directions be represented by indices 1, 2, and 3, respectively. Then, the composite specimen with straight fibers aligned in the x direction is characterized by nine elastic constants: C_{11}, C_{22}, C_{33}, C_{12}, C_{13}, C_{23}, C_{44}, C_{55}, and C_{66}.

Consider a small element of the wavy composite at a typical local point (x, y_0, z_0). The small local element is considered to have orthorhombic symmetry whose x and y symmetry axes are rotated about the third symmetry axis z_0z by the angle β_f from the x axis. Let's specify a wave normal **n** of the wave propagating in the xy plane by an angle θ mea-

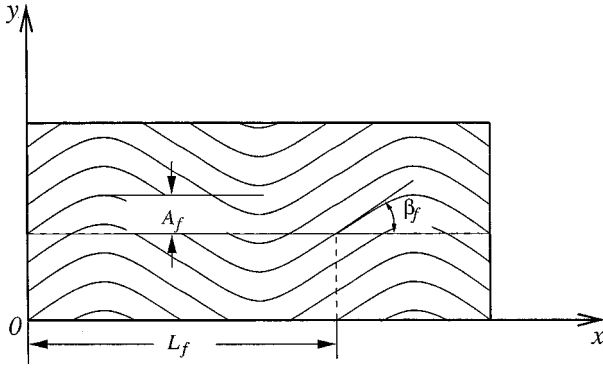[a]Electronic mail: kykim@msc.cornell.edu

FIG. 1. Schematics of a wavy fiber composite specimen.

sured from the x axis. Then, the angle α which the wave normal $\mathbf{n}$ makes from the local fiber direction is

$$\alpha(x,\theta) = \theta - \beta_f = \theta - \tan^{-1}\left(\frac{2\pi A_f}{L_f}\cos\frac{2\pi x}{L_f}\right). \quad (3)$$

We invoke Snell's law and the formulas for the arrival time τ and ray path of a wave initiating from the point (x_0, y_0, z_0) and arriving at the point (x_1, y_1, z_0). Referring to the results established in the geometrical acoustics of inhomogeneous anisotropic media,[5,6] they can be written as

$$h = \frac{\sin\theta_0}{v_0} = \frac{\sin\theta}{v} = \text{constant}, \quad (4)$$

$$\tau = \int_{x_0}^{x_1} \frac{dx}{v\cos\theta - v'\sin\theta}, \quad (5)$$

$$y_1 = y_0 + \int_{x_0}^{x_1} \frac{v\sin\theta + v'\cos\theta}{v\cos\theta - v'\sin\theta}\,dx, \quad (6)$$

where $v(x,\theta)$ is the phase velocity and $v' = \partial v/\partial\theta$.

For the waves propagating in the xy plane, the eikonal and phase velocity equations are factored into three modes whose vibration directions are mutually perpendicular to each other: shear horizontally (SH) polarized pure transverse (PT) mode vibrating in the z direction, quasilongitudinal (QL) mode and quasitransverse (QT) mode. The QL and QT modes are both polarized in the xy plane. The SH polarized PT mode is uncoupled from the QL and QT modes. We first deal with the PT mode.

A. Pure transverse mode

The phase velocity v of the PT mode is given by[7]

$$\rho v^2 = C_{44}\sin^2(\theta - \beta_f) + C_{55}\cos^2(\theta - \beta_f), \quad (7)$$

which we differentiate with respect to θ to obtain

$$\rho v v' = (C_{44} - C_{55})\sin(\theta - \beta_f)\cos(\theta - \beta_f). \quad (8)$$

Using Snell's law Eq. (4), Eq. (7) is expressed as

$$\rho\sin^2\theta = h^2[C_{44}\sin^2(\theta - \beta_f) + C_{44}\cos^2(\theta - \beta_f)]$$

$$= h^2[(C_{44} - C_{55})\sin^2(\theta - \beta_f) + C_{55}], \quad (9)$$

where $h = \sin\theta/v$ is the constant in Snell's law. Consider a case in which rays are initiating from a broadband source in

virtually every direction inside the specimen. We choose an arbitrary ray whose wave normal at the source is directed at an angle θ_0 from the x direction. The fiber direction β_f at the source is obtained from Eq. (2). Then, we calculate the initial velocity v_0 corresponding to the wave normal θ_0 via Eq. (7) to determine the Snell's law constant h from Eq. (4). For a given x, the fiber angle β_f can be calculated via Eq. (2) and from Eq. (9), one obtains the solutions for θ, $\sin\theta$, and $\cos\theta$. Then the values of v and v' are obtained from Eqs. (7) and (8). Thus, one can calculate the values of $\sin\theta$, $\cos\theta$, and v and v' at many different values of x to determine the arrival time τ and ray path through Eqs. (5) and (6). One can repeat this procedure for rays with various initial wave normal directions.

For the special case of the initial wave normal $\mathbf{n}$ pointing in the x direction, $h = \sin\theta/v = 0$, i.e., $\theta = 0$ all along the ray path, and the arrival time and ray path integrals are simplified to

$$\tau = \rho\int_{x_0}^{x} \frac{dx}{[(C_{44} - C_{55})\sin^2\beta_f + C_{55}]^{1/2}}, \quad (10)$$

$$y - y_0 = \int_{x_0}^{x} \frac{(C_{55} - C_{44})\sin\beta_f\cos\beta_f}{C_{44}\sin^2\beta_f + C_{55}\cos^2\beta_f}\,dx$$

$$= \frac{C_{55} - C_{44}}{C_{44}}\frac{L_f^2}{4\pi^2 A_f\,p}$$

$$\times\tanh^{-1}\frac{p[\sin(2\pi x/L_f) - \sin(2\pi x_0/L_f)]}{p^2 - \sin(2\pi x_0/L_f)\sin(2\pi x/L_f)}, \quad (11)$$

where

$$p = \sqrt{1 + \frac{L_f^2 C_{55}}{4\pi^2 A_f^2 C_{44}}}. \quad (12)$$

Equation (11) indicates that the ray with initial wave normal $\mathbf{n}$ directed along the x-axis follows a path with the same periodic length that the wavy fiber has.

B. Quasilongitudinal and quasitransverse modes

For simplicity of notation we introduce the following identities

$$C_{11\pm} = C_{11} \pm C_{66}, \quad C_{22\pm} = C_{22} \pm C_{66}, \quad C_{12\pm} = C_{12} \pm C_{66}. \quad (13)$$

The phase velocities of the QL and QT modes are given by[7]

$$2\rho\,v^2 = C_{11+}\cos^2\alpha + C_{22+}\sin^2\alpha \pm \sqrt{D}, \quad (14)$$

where α is defined in Eq. (3), the upper and lower signs in $\pm$ in front of $\sqrt{D}$ correspond to the QL and QT modes, respectively, and

$$D = (C_{11-}\cos^2\alpha - C_{22-}\sin^2\alpha)^2 + 4C_{12+}^2\sin^2\alpha\cos^2\alpha. \quad (15)$$

Differentiating Eq. (14) with respect to θ, one obtains

$$\frac{v'}{v} = \frac{1}{4\rho v^2}\left\{(C_{22+} - C_{11+})\sin 2\alpha \pm \frac{1}{\sqrt{D}}\right.$$

$$\times [(C_{22-}\sin^2\alpha - C_{11-}\cos^2\alpha)(C_{11-} + C_{22-})$$

$$\left.\times \sin 2\alpha + C_{12+}^2\sin 4\alpha]^{1/2}\right\}. \tag{16}$$

Substitution of Snell's law Eq. (4) into Eq. (14) yields

$$2\rho\,\sin^2\,\theta = h^2[C_{11+}\cos^2(\theta - \beta_f) + C_{22+}\sin^2(\theta - \beta_f) \pm \sqrt{D}]. \tag{17}$$

Determination of the arrival time and ray path of a wave with initial wave normal θ_0 at the source can be carried out in a similar way to that described in the case of the PT mode. In the special case of $h = \sin\theta = 0$, the evaluation of the integrals for the arrival time and ray path is also simplified as in the PT mode.

II. EXPERIMENTAL METHOD

Two kinds of specimens are fabricated using graphite-fiber prepregs: one is a unidirectional, straight graphite fiber–epoxy composite and the other is a wavy graphite fiber–epoxy specimen with sine wave period 40 mm and wavy amplitude 2 mm. Both specimens have the same density 1524 kg/m^3. The straight fiber direction in the unidirectional composite and the mean fiber direction in the wavy composite are taken as the x direction. The wavy fiber plane is denoted as the xy plane.

In order to fabricate the wavy composite, the top surface of an aluminum plate, which is 20 cm wide, 60 cm long, and 12.7 mm thick, is first machined in the desired sine wave pattern (2 mm amplitude and 40 mm period) on a numerically controlled machine. Then, the machined aluminum plate is split into two identical pieces, which are next aligned against each other with a gap, where many layers of graphite–fiber epoxy prepregs are sandwiched and cured.

The unidirectional composite, which is weakly orthorhombic, is prepared to determine its nine elastic constants from measurements of the travel times of ultrasonic waves propagating through the specimen. A cube of the unidirectional composite which has been cut perpendicular to the three symmetry axes is mechanically polished. The PT waves are launched from one side of the specimen and they are detected on the opposite side, while the PL (pure longitudinal) waves are generated and detected by the same transducer. Denoting the propagation and polarization directions of the phase velocity v of an ultrasonic wave by subscript indices i and j, respectively, the pure index elastic constants or the diagonal elements of C_{ij} matrix are expressed as

$$\rho[v_{ij}^2] = \begin{bmatrix} C_{11} & C_{66} & C_{55} \\ C_{66} & C_{22} & C_{44} \\ C_{55} & C_{44} & C_{33} \end{bmatrix}. \tag{18}$$

Thus, all six pure index elastic constants can be determined via Eq. (18) from the phase velocity measurements along the three symmetry directions. Given the values of the pure-index elastic constants, the mixed index elastic constant $C_{ij}\;(i \neq j)$ can be obtained from the wave speed measurements of the QL mode propagating in an oblique direction in the symmetry plane. For this purpose two opposite faces of three additional specimens cut from the large unidirectional composite are polished with one in 45° to the x axis and normal to the xy plane, another in 45° to the y axis and normal to the yz plane, and the other in 45° to the z axis and normal to the zx plane. From the measurement of the QL phase velocity propagating in 45° direction to the x axis in the xy plane, one uses Eq. (14) by setting $\beta_f = 0$ and $\theta = 45°$ to obtain the mixed index elastic constant C_{12}. One proceeds similarly for determination of C_{13} and C_{23}, using the other two obliquely cut specimens. The nine elastic constants of the orthorhombic unidirectional composite can also be determined from the group velocity measurements and this is described in detail elsewhere.[8,9]

One of the fabricated wavy composites has two opposite sides machined flat, which are normal to the wavy fiber plane and parallel to the x axis. It has next been polished with thickness 15.93 mm between the flat surfaces. Then another sample is prepared with two flat opposite faces normal to the x axis with thickness 30 mm between them. A schematic of a typical sample is shown in Fig. 1. First, a 28 μm thick, piezoelectric polyvinylidene fluoride (PVDF) film is laid on the top surface of the flat wavy composite and a glass capillary of size 0.10 mm inside diameter and 0.17 mm outside diameter is mounted on the PVDF film. Pointlike sources of the QL and QT modes are generated by breaking the glass capillary with a razor blade at various x positions on the top surface. The generated elastic waves propagate in virtually every direction inside the specimen and are detected at various x positions on the bottom surface by a pointlike piezoelectric detector of 0.75 mm diameter. The output of the PVDF film indicates a time of source generation and serves as a trigger for the output of the piezoelectric detector. From the arrival-time difference between the two signals, the travel time of the QL mode is determined. Identification of the QL ray arrival in a detected signal is easy, because the arrival is found at the point from which the signal first jumps from noise level. The QT mode in the detected signal is very difficult to identify and we did not attempt to measure its arrival time.

For measurements of the arrival times of the PT mode propagating on the xy wavy fiber plane, a line-type piezoelectric shear transducer, whose active area is 0.75 mm wide and 5 mm long, is mounted on the bottom face of the specimen at different x positions with its polarization aligned along the z direction. The polarization direction of the shear transducer is along the 5 mm lengthwise direction. It generates not only QL modes but also shear horizontally (SH) polarized pure transverse (PT) mode propagating along virtually every direction on the xy plane. The propagated PT modes are detected by a small piezoelectric shear transducer with active area of 0.75 mm diameter, which is attached on the various x positions of the top surface with its polarization aligned along the z direction. Identification of the PT mode arrival in the detected signals that travel through composite materials is not so easy, because its arrival trails that of the QL mode. How to identify the arrival time of the SH polar-
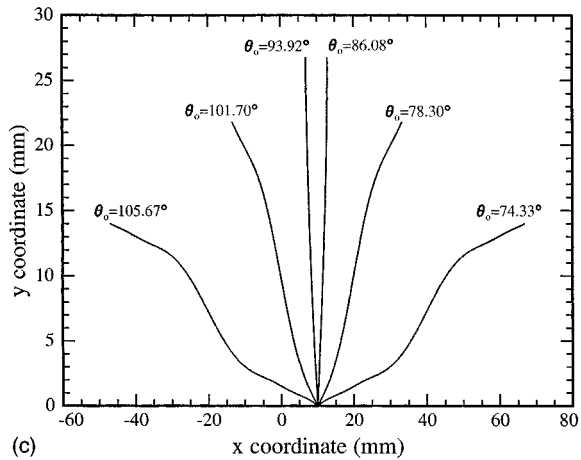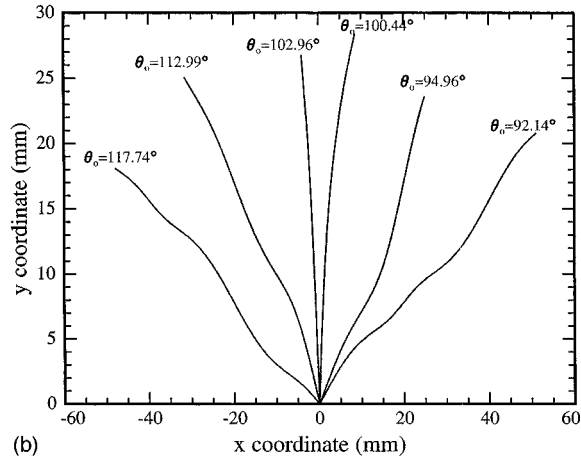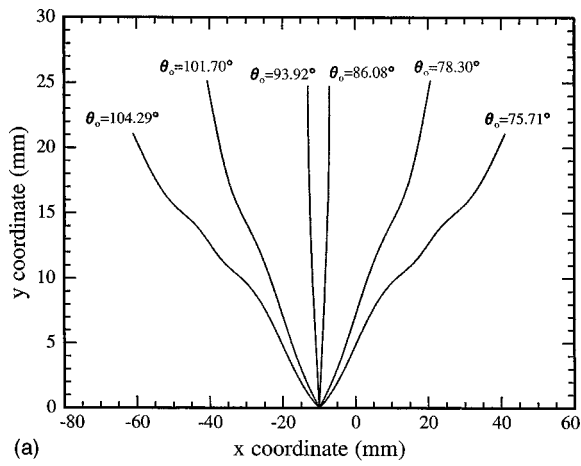
2298 J. Acoust. Soc. Am., Vol. 103, No. 5, Pt. 1, May 1998

Kim *et al.*: Waves in a wavy composite 2298

FIG. 2. Ray paths of the QL mode with sources at (a) $x = -10$ mm, (b) $x = 0$ mm, and (c) $x = 10$ mm.

FIG. 3. Ray paths of the PT mode with sources at (a) $x = -10$ mm, (b) $x = 0$ mm, and (c) $x = 10$ mm.

ized PT mode in the detected signal is described in Ref. 9.

It is noted that both the capillary fracture source and piezoelectric detector used for the QL mode have a frequency bandwidth extending well above 10 MHz, while both piezoelectric source and detector used for the PT mode have a broadband frequency spectrum which is centered around 5 MHz. These correspond to a wavelength of the QL mode less than 1 mm and that of the PT mode less than 0.2 mm. These wavelengths are much less than the wavy period of the composite, 40 mm and one expects that a high-frequency geo-
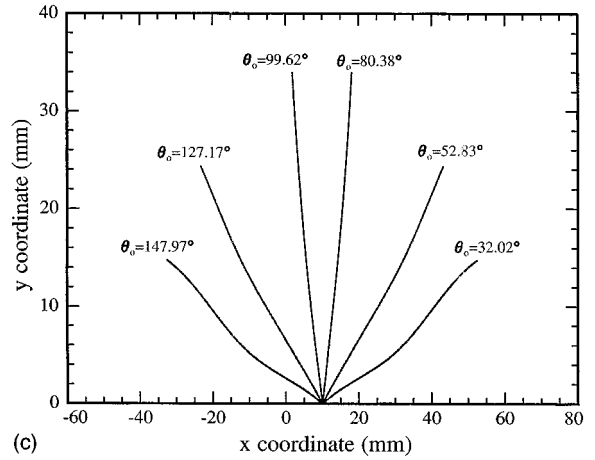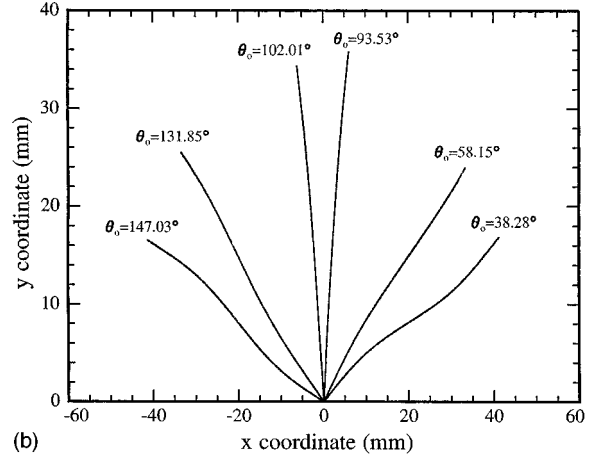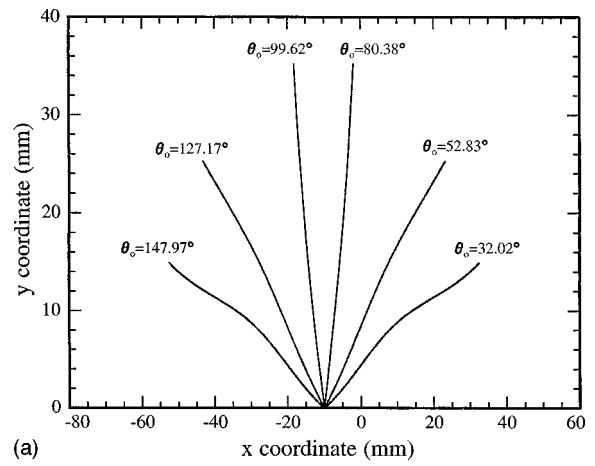
metrical acoustics approximation would hold well in describing the propagation of wave fronts.

III. RESULTS

The obtained nine elastic constants of the unidirectional composite in units of GPa are: $C_{11} = 130.3 \pm 1.5$, $C_{22} = 11.00 \pm 0.28$, $C_{33} = 12.46 \pm 0.44$, $C_{44} = 2.95 \pm 0.08$, $C_{55} = 5.47 \pm 0.22$, $C_{66} = 4.96 \pm 0.08$, $C_{12} = 6.01 \pm 0.36$, $C_{13} = 1.04 \pm 0.09$,
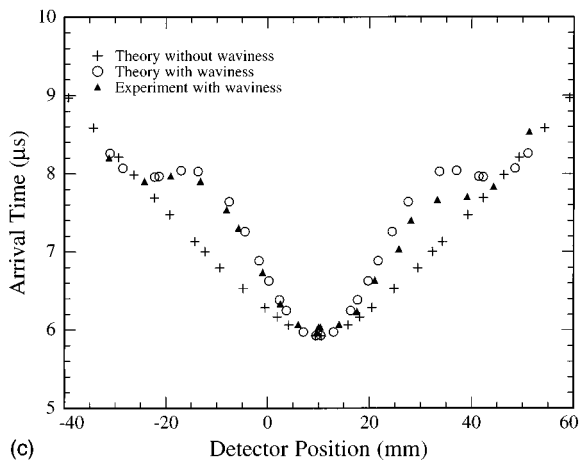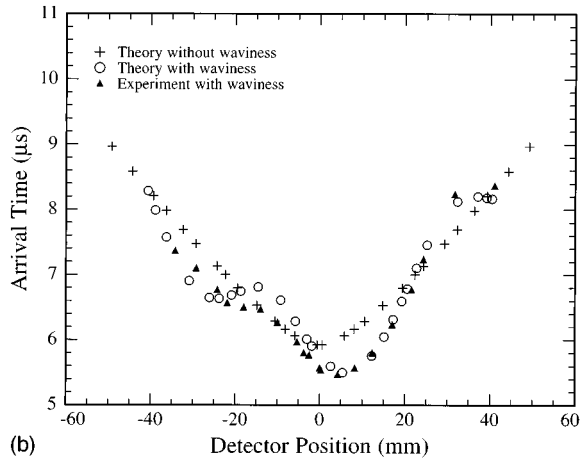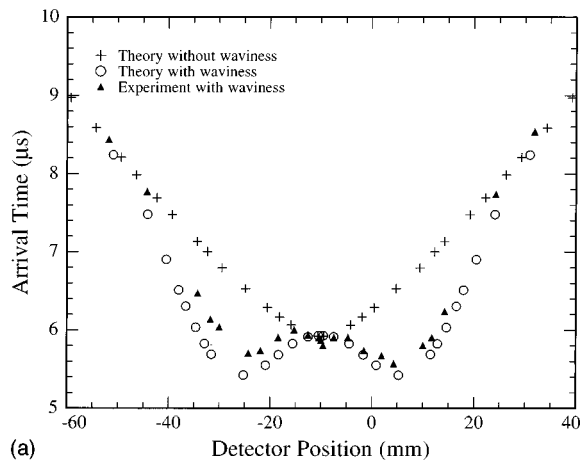
(a)

(b)

(c)

FIG. 4. Comparison of predicted arrival times of the QL ray with measured values. (a) Source at $x = -10$ mm, (b) source at $x = 0$ mm, and (c) source at $x = 10$ mm.

and $C_{23} = 6.27 \pm 0.37$. We recall that the density and thickness of the wavy composite specimen are 1524 kg/m^3 and 15.93 mm, respectively.

Using these data, the ray paths of the QL mode with sources at $x = -10$, 0, and 10 mm on the bottom face are plotted in Fig. 2(a), (b), and (c), respectively. Those of the PT mode with sources at the same x positions are displayed in Fig. 3(a), (b), and (c), respectively. Although the capillary fracture QL sources are located on the top surface of the wavy composite, the ray paths are drawn as if they were
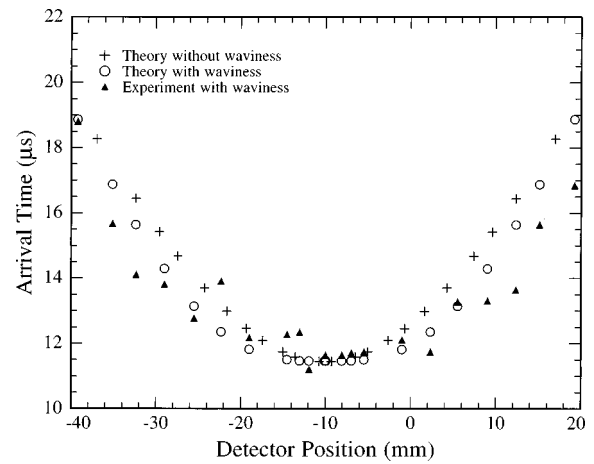

FIG. 5. Comparison between predicted arrival times of the PT ray with a source at $x = -10$ mm and measured values.

located on the bottom surface, which is given the coordinate of $y = 0$. As expected, the ray paths of both QL and PT modes with the sources at $x = -10$ and 10 mm exhibit a symmetry pattern about the y axis passing through the source, while the symmetry is broken for the ray paths with a source at $x = 0$ mm. θ_0 in these figures indicates the direction of the wave normal associated with a particular ray at the source point. Note that the rays are not only curved but also multiply curved for those substantially away from the vertical direction. QT ray paths are not plotted, because they can be refracted into QL modes anywhere on their path and the arrival of the QT rays are almost impossible to identify in the detected signals.

Comparison of theory with experiment on the ray arrival times of the QL mode is displayed in Fig. 4(a), (b), and (c) with sources at $x = -10$, 0, and 10 mm, respectively. Theoretical values of arrival times in a straight unidirectional fiber composite of the same thickness with similar source-to-detector configurations are also drawn with + (plus) symbols to elucidate the effect of fiber-waviness. It is seen that predicted values generally agree well with experimentally observed values. This signifies that the geometrical acoustics developed for a heterogeneous anisotropic medium provides a good approximation to the travel times of ultrasonic rays and it can be applied to the study of wave propagation in the wavy composite. It also indicates that geometrical acoustics, which is a high-frequency approximation, remains quite valid in the ultrasonic frequency range for description of wave front behavior in a wavy composite material. The deviations of predicted values from measured travel times at some detector positions are likely to be a result of rays passing through a local region where fiber arrangement deviates from the regular wavy pattern before the rays arrive at the detector. As expected, the QL ray arrival times with sources at $x = -10$ and 10 mm exhibit symmetry about their source positions. It is, however, interesting to see that the symmetry patterns are quite different in two cases.

Predicted arrival times of the PT mode are compared with measured values in Fig. 5. Theoretical arrival times in a corresponding straight fiber composite without waviness are also drawn with + (plus) symbols for comparison. The mea-
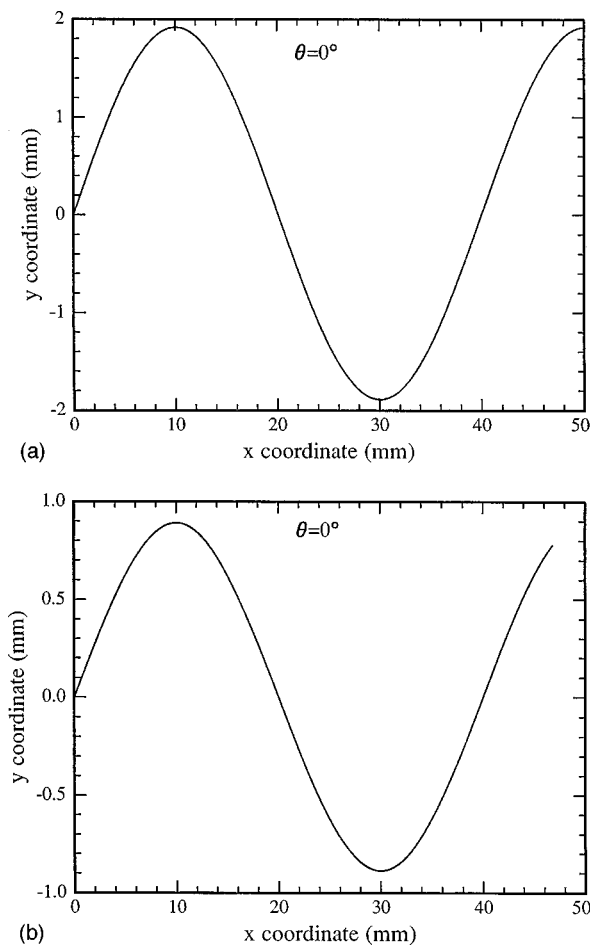
(a)

(b)

FIG. 6. The path of a ray initiating from origin with wave normal pointing in the x direction. (a) QL mode and (b) PT mode.

sured arrival times exhibit symmetry about the y axis that passes a source located at $x = -10$ mm, but they are more scattered than those of the observed QL mode. This is partly due to the difficulty of correctly identifying the PT mode arrival and as a result, the measured arrival times are considered approximate values with several % error.

Finally, the ray paths of the QL and PT modes initiating at origin ($x = 0$ mm, $y = 0$ mm) with initial wave normal pointing in the x direction are plotted in Fig. 6(a) and (b), respectively. In this case the direction of wave normal is constant, always in the x direction, all along the ray path, as Snell's law Eq. (4) implies. As can be seen from Fig. 6(a) and (b), both ray paths have the same periodic length as the wavy fiber has, but they have different amplitudes. In the case of the PT mode, this result is already predicted by Eq. (11). It is interesting to notice that the ray path of the QL mode with wave normal in the x direction closely follows a wavy fiber, while that of the PT mode deviates somewhat from the wavy fiber. One finds in Fig. 6(a) that the y coor-

dinate of the QL ray at $x = 30$ mm is -1.89 mm. We have prepared a specimen with two parallel sides terminating at $x = 0$ mm and $x = 30$ mm. The measured arrival time of the QL mode at the point ($x = 30$ mm, $y = -1.89$ mm) with a source at origin is 3.33 μs, which agrees remarkably well with the predicted value 3.32 μs.

IV. CONCLUSIONS

We have established closed-form analytic solutions for the ray path and travel time of the QL, QT, and PT rays propagating in a wavy fiber composite. Predicted values of travel time of QL and PT modes are in good agreement with experimentally observed values. Geometrical acoustics developed for a heterogeneous anisotropic material can be useful for investigation of a wavy composite material. We have also shown that a high-frequency geometrical acoustics approximation holds well in the ultrasonic frequency range in describing the propagation of wave fronts in a wavy fiber composite. The method used in this paper may well be adapted to investigating wave propagation in various inhomogeneous anisotropic structures, such as devices with gradient of material properties (e.g., diffused concentration), depth-dependent media, and structures of inhomogeneous stress field, etc.

ACKNOWLEDGMENTS

[1] A. L. Highsmith, J. J. Davis, and K. L. E. Helms, "The influence of fiber waviness on the compressive behavior of unidirectional continuous fiber composites," in *Composite Materials: Testing and Design,* Vol. 10, ASTM STP 1120, edited by G. C. Grimes (ASTM, Philadelphia, 1992), pp. 20–36.

[2] H. M. Hsiao, I. M. Daniel, and S. C. Wooh, "Effect of fiber waviness on the compressive behavior of thick composites," in *Failure Mechanics in Advanced Polymeric Composites,* AMD-Vol. 196 (ASTM, Philadelphia, 1994), pp. 141–159.

[3] S. C. Wooh and I. M. Daniel, "Wave propagation in composite materials with fiber waviness," Ultrasonics **33**, 3–10 (1995).

[4] J. S. McIntyre, C. W. Bert, and R. A. Kline, "Wave propagation in a composite with wavy reinforcing fibers," in *Review of Progress in Quantitative Nondestructive Evaluation,* Vol. 14, edited by D. O. Thompson and D. E. Chimenti (Plenum, New York, 1995), pp. 1311–1318.

[5] N. J. Vlaar, "Ray theory for an anisotropic inhomogeneous medium," Bull. Seismol. Soc. Am. **58**, 2053–2072 (1968).

[6] V. Cerveny and I. Psencik, "Rays and travel time curves in inhomogeneous anisotropic media," Z. Geophys. **38**, 565–577 (1972).

[7] M. J. P. Musgrave, *Crystal Acoustics* (Holden-Day, San Francisco, 1970).

[8] K. Y. Kim, "Analytic relations between the elastic constants and the group velocity in an arbitrary direction of symmetry planes of media with orthorhombic or higher symmetry," Phys. Rev. B **49**, 3713–3724 (1994).

[9] K. Y. Kim, R. Sribar, and W. Sachse, "Analytical and optimization procedures for determination of all elastic constants of anisotropic solids from group velocity data measured in symmetry planes," J. Appl. Phys. **77**, 5589–5600 (1995).